Microelectronic Engineering 91 (2012) 39–43

Contents lists available at SciVerse ScienceDirect

Microelectronic Engineering

journal homepage: www.elsevier.com/locate/mee

Arrays of nano-structured surfaces to probe the adhesion and viability of bacteria

Andras Z. Komaromy [a], Shuyan Li [a], Hailong Zhang [a], Dan V. Nicolau [a,b], Reinhard I. Boysen [a,*], Milton T.W. Hearn [a]

[a] ARC Special Research Centre for Green Chemistry, Monash University, Clayton, VIC 3800, Australia
[b] Department of Electrical Engineering and Electronics, The University of Liverpool, Brownlow Hill, Liverpool L69 3GJ, UK

ARTICLE INFO

Article history:
Received 13 September 2010
Received in revised form 28 October 2011
Accepted 28 October 2011
Available online 10 November 2011

Keywords:
Nanostructures
e-Beam lithography
Bacterial adhesion
Staphylococcus aureus
Escherichia coli

ABSTRACT

Nano-structured silicon wafers with arrays of dots and lines of different width and pitch were manufactured by e-beam lithography. The resulting arrays were composed of 50 × 50 μm fields. These arrays consisted of either dots (gold) of different width (400–800 nm) and pitch (500–1000 nm) or lines (gold) of different width (100–1000 nm) and pitch (200–1200 nm) and were characterised by atomic force microscopy. The wafers were incubated with bacterial suspensions under their optimal physiological conditions and carefully rinsed. The surfaces were then treated with a fluorescent cell viability stain and the remaining bacteria were imaged with a fluorescence microscope in the reflectance mode to count the number of live and dead cells on the array fields. The results confirm that the cell survival and adhesion was influenced by a combined effect of bacterial size, physiology and array surface topography. These investigations provide insights that may be useful for the manufacturing of 'designer' materials with pro- or anti-bacterial properties.

1. Introduction

The design and manufacture of nanostructured surfaces with defined topography and chemical functionality provides excellent opportunities to generate novel pro- or anti-bacterial surfaces for lab-on-a-chip systems, miniaturised bioreactors or medical devices. Bacterial cell adhesion, an important step in biofilm formation, can be influenced by a variety of physico-chemical and topographical features associated with the interfacial contacts made between a bacterium and a surface [1–3]. Recently, we used microstructure arrays on silicon wafers manufactured by optical lithography to investigate their effect on bacterial cell viability and attachment [4]. These micro-structure arrays had been coated with gold and were further modified through direct self-assembly processes with 11-mercapto-1-undecanol or 1-undecanethiol, resulting in respectively hydrophilic or hydrophobic self-assembled monolayer surfaces. Cell viability and adhesion was found to be influenced by a combined effect of the zeta-potential of the surface (when compared to that of the bacterium) and surface topography of the micro-structure array. Although bacterial adhesion and biofilm formation has been documented in the literature for a variety of different surfaces [5–10], bacterial behaviour on nano-structured surfaces has so far not been systematically explored. In this study, we have investigated the effects of surface nano-topography on the attachment and viability of two bacterial species, namely *Escherichia coli* and *Staphylococcus aureus.* The use of nano-structured arrays has the advantage of allowing the simultaneous rapid screening of the effects of different topographies on the adhesion of the same or different bacterial strains under similar conditions, which is difficult to achieve when individual surfaces are screened separately due to the variability in handling conditions, and the possibilities for non-equivalence in the number of colony forming units per mL or non-comparability in the bacterial growth kinetics over time.

2. Methodology

2.1. Manufacturing of nano-structures

Nano-structured arrays were manufactured on silicon wafers by e-beam lithography at the Instituto Microelectronica (Barcelona, Spain). A 100 nm thick layer of a positive electron beam lithographic resist (poly-methyl methacrylate, PMMA 950 k) was deposited by spin-coating on top of an oxidised silicon chip. This layer was then subjected to e-beam lithography and development to locally remove the PMMA to form a dot or line pattern. Subsequently, a 35 nm thick gold-on-chromium (30 nm/5 nm) layer was deposited over the entire chip by e-beam evaporation; the remainder of the PMMA was then removed with acetone, resulting in an oxidised silicon surface interrupted by gold protrusions in form of dots or lines (Fig. 1A). These nano-structured surfaces had either gold dots with a height of 35 nm or lines of 35 nm height on 50 × 50 μm^2 areas. Array 1 (dot pattern) was manufactured with a dot diameter (width,

* Corresponding author. Tel.: +61 3 9905 4516; fax: +61 3 9905 8501.
E-mail address: reinhard.boysen@monash.edu (R.I. Boysen).

0167-9317/$ - see front matter © 2011 Elsevier B.V. All rights reserved.
doi:10.1016/j.mee.2011.10.012

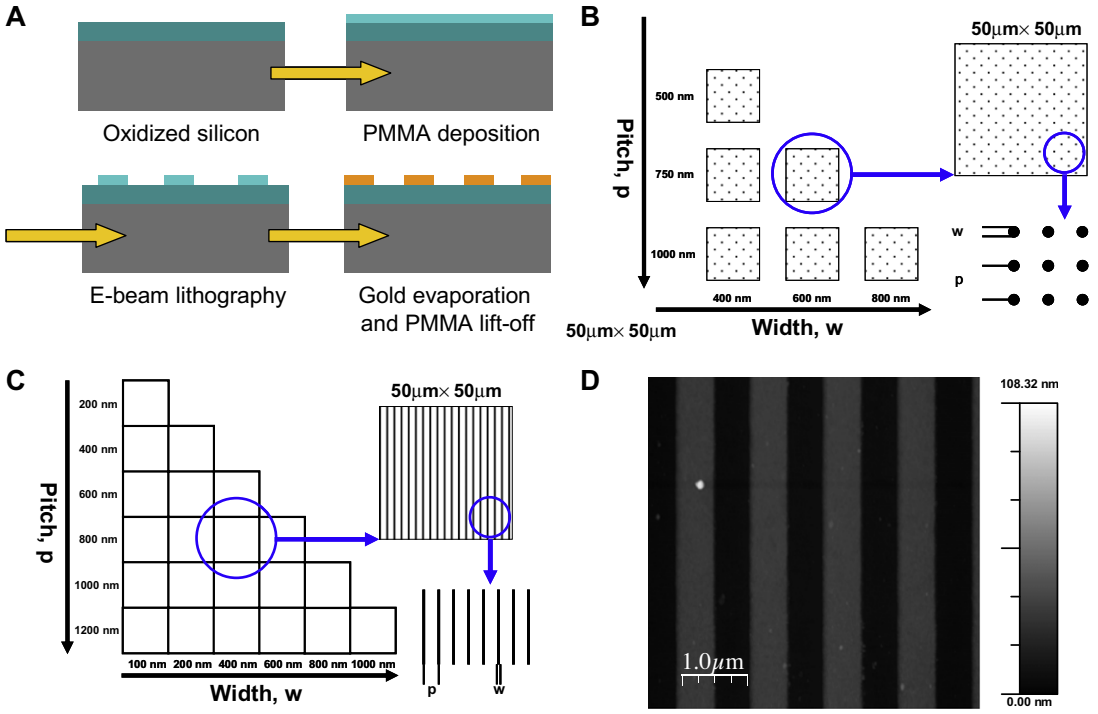

Fig. 1. Steps to manufacture nanostructured surfaces. (A) A silicon wafer was subjected to oxidation, poly-methyl methacrylate (PMMA) deposition, e-beam lithography, gold deposition and PMMA lift-off. (B) Scheme of dot array containing fields of dots with varying dot widths and pitch. (C) Scheme of line array with fields of lines of different line widths and pitch. The height of the structures was 35 nm. (D) Atomic force microscopy image of a section of a field of gold lines on silicon oxide with a width of 600 nm and pitch of 400 nm. (For interpretation of the references to colour in this figure legend, the reader is referred to the web version of this article.)

w) of 200 nm, 400 nm and 600 nm and a pitch (*p*) of 500 nm, 750 nm and 1000 nm (Fig. 1B). Array 2 (line pattern) was manufactured with a nominal line width of 100 nm, 200 nm, 400 nm, 600 nm, 800 nm and 1000 nm, and a nominal pitch of 200 nm, 400 nm, 600 nm, 800 nm, 1 μm and 1.2 μm (Fig. 1C). Structures were subjected to defectivity analysis with atomic force microscopy prior to use.

2.2. Bacterial cell culture and exposure to nanostructures

E. coli BL21 (ATCC 11303) and *S. aureus* (ATCC 6538), obtained from the Department of Microbiology, Monash University, Melbourne, Australia, were selected as representative species, as they have the cell wall characteristics of gram-negative and gram-positive bacteria, respectively. *E. coli* was grown in LB medium and *S. aureus* in 2YT medium. One litre LB medium contained 10 g tryptone (pancreatically digested casein, Merck, Darmstadt, Germany), 5 g yeast extract (Merck, Darmstadt, Germany) and 10 g NaCl (Amresco, Solon, OH, USA). One litre 2YT medium contained 16 g tryptone, 10 g yeast extract and 5 g NaCl. The pH of all media was adjusted to 7.2. Cells were grown until they reached the mid-log phase, centrifuged and the pellets were resuspended in phosphate buffer to adjust the final cell concentration to $1-3\times10^8$ colony forming units/mL. All nano-structured wafers as well as the planar reference surfaces were incubated in the cell suspensions for 2 h, washed twice with phosphate buffer and ultra pure water and air-dried at room temperature. Time course incubation experiments of *E. coli* and *S. aureus* with planar gold surfaces (Arrandee, Werther, Germany) were performed from 15 min to 2 h 30 min.

2.3. Fluorescence staining and microscopy

The nano-structured silicon wafers, after having been incubated with the bacterial solutions, were soaked in a solution of LIVE/DEAD *BacLight* bacterial viability fluorescent dye (Invitrogen Pty Ltd., Melbourne, Australia) for 15 min and washed with sterile ultra pure water, dried and investigated with an Olympus BX51 fluorescence microscope (Olympus Corporation, Tokyo, Japan) in the reflectance mode. Images were taken in fluorescent mode using a U-MWB2 cube for live and a U-MWG2 cube for dead cells or in the differential interference contrast (DIC) mode with a digital Spot R3 camera (Diagnostic instruments, Inc., Sterling Heights, MI, USA). Image and data processing were carried out with the Image-Pro Plus 6.0 software (Media Cybernetics, Inc., Silver Spring, MD, USA) to count the numbers of live and dead bacteria in triplicate measurements. To enable comparison, the cell numbers were expressed per 100 μm^2.

2.4. Surface analysis

Surface characterisation was undertaken in air with a PicoPlus atomic force microscope (AFM) interfaced with a Picoscan 3000 controller (both from Molecular Imaging Inc., USA). A silicon cantilever (Ultrasharp, NSC15/AIBS, MikroMasch) was used with a typical spring constant of 40 N/m in tapping mode. The resulting images were analysed using software WS×M 4.0 Develop 11.6.

3. Results and discussion

In this investigation, e-beam lithography was successfully used to produce arrays with gold/silicon oxide nano-structures in the form of dots and lines of different sizes and with different spacings. An AFM image of a subsection of a field of lines is shown in Fig. 1D. To assess the propensity of bacterial cells to adhere to these arrays of nano-structures, these new materials as well as the planar reference surfaces were incubated with suspensions of *E. coli* and *S. aureus*. Examples of differential interference contrast microscopy (DIC) images of live *S. aureus* cells on dot and line gold/silicon oxide nano-structured surfaces are shown in Fig. 2. With DIC methods,

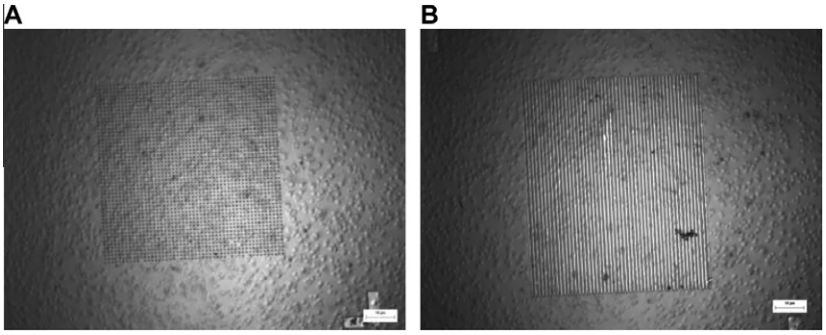

Fig. 2. Differential interference contrast microscopy (DIC) images of live *S. aureus* cells on gold/silicon oxide nano-structured surfaces. (A) Dots with a width of 600 nm and a 1000 nm pitch and (B) lines width of 400 nm and a 1000 nm pitch. The bar represents 10 μm.

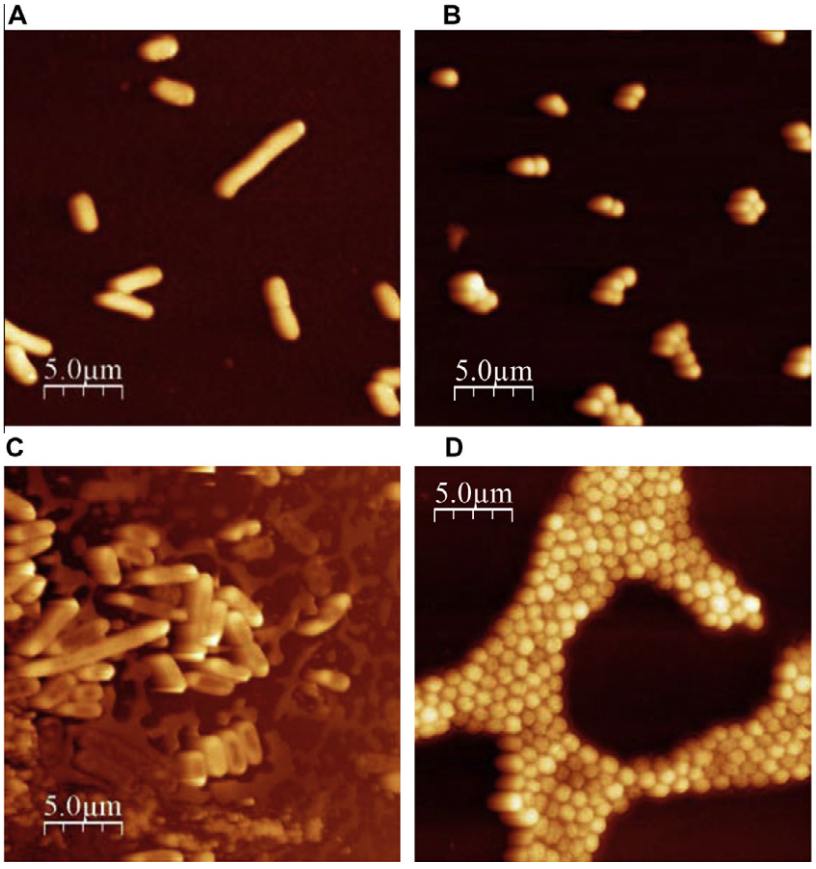

Fig. 3. Atomic force microscopy image of *E. coli* (A, C) and *S. aureus* (B, D) cells on planar gold surfaces after 15 min (A, B) and 2 h (C, D) incubation time.

the images of bacterial cells adherent to dot or line gold/silicon oxide nano-structured surfaces can be reliably acquired ensuring that cell damage or distortion, due to handling artefacts that may arise with AFM methods, has not occurred. After staining with bacterial viability fluorescent dye the number of live and dead bacterial cells was independently counted when imaged by fluorescence microscopy in the reflectance mode.

On planar gold surfaces at short incubation times, i.e., $\leqslant$15 min, *E. coli* appeared as single or dividing cells (Fig. 3A), whilst *S. aureus* appeared to form cell clusters (Fig. 3B). At longer incubation times, i.e., $\geqslant$2 h the population density of *E. coli* cells increased (Fig. 3C), whilst *S. aureus* formed a biofilm (Fig. 3D).

On the dot nanostructures of array 1, ($50 \times 50\ \mu m^2$) with a dot width of 600 nm and a 1000 nm pitch (Fig. 4) at 2 h incubation time, live *E. coli* preferentially colonised the nanostructures over the surrounding silicon surface, with the resultant generation of patches of both live and dead cells. The number of cells per each 100 μm^2 were live *E. coli* 5.67 (S.D. 0.58) (Fig. 4A) and dead *E. coli* 3.33 (S.D. 1.55) (Fig. 4C), respectively, whilst the corresponding unstructured silicon surfaces each only yielded 1.33 (S.D. 0.58) bacteria. In contrast, live *S. aureus* (Fig. 4B) populated the nanostructured surface as single cells not forming a biofilm on planar gold surfaces, with a cell number for 100 μm^2 of 9.67 (S.D. 0.58) and the surrounding silicon surface with 6.33 (S.D. 1.15) cells. There were very few dead cells (1.33, S.D. 0.58) (Fig. 4D) on the nanostructure and 1 (S.D. 0) outside.

The line nanostructures of array 2 ($50 \times 50\ \mu m^2$) had a similar effect on the adhesion of both bacteria. Exemplary fluorescence microscopy images of live and dead *E. coli* showed the number of cells per 100 μm^2 to be 3.25 (S.D. 1.71) and 5.0 (S.D. 1.83), respec-

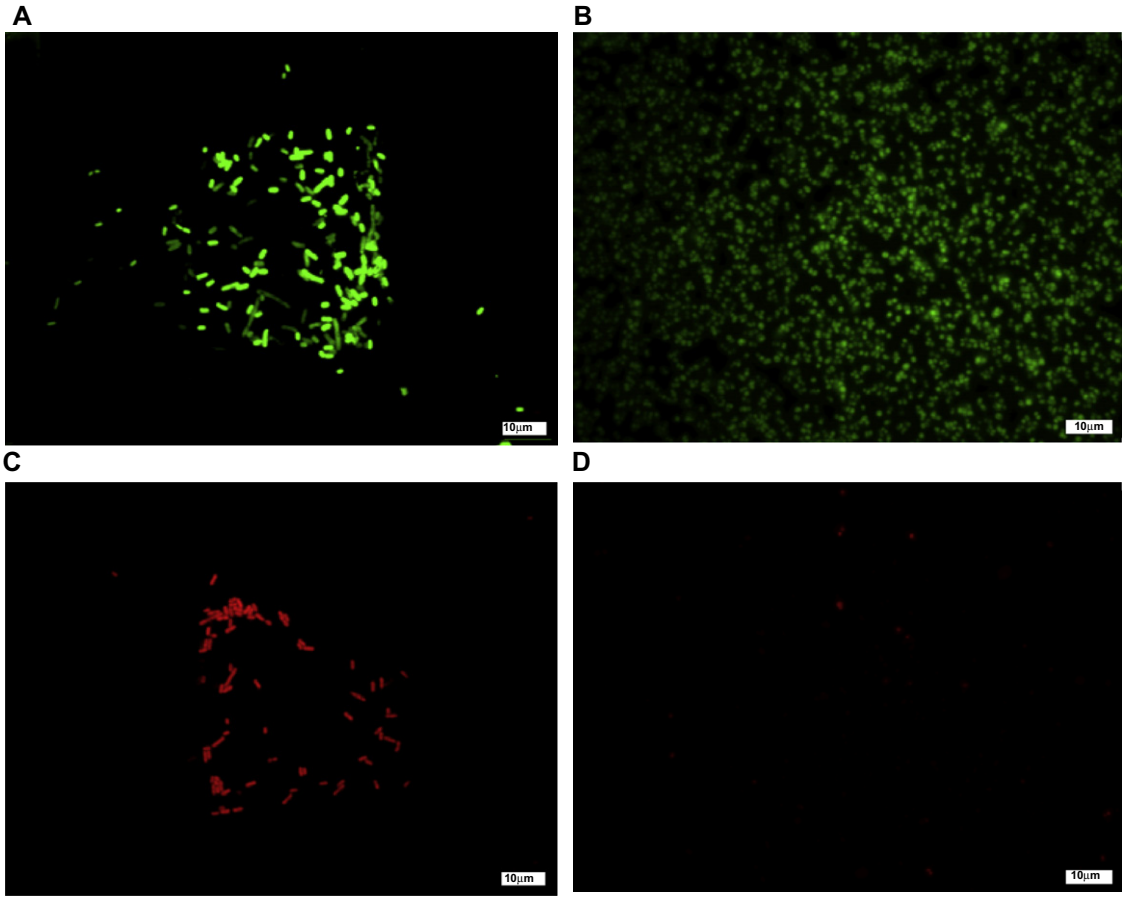

Fig. 4. Fluorescence microscopy images of live (A) and dead (C) *E. coli* and live (B) and dead (D) *S. aureus* cells after bacterial viability staining on gold/silicon oxide dot-nanostructures of 50 × 50 μm^2 with a dot width of 600 nm and a 1000 nm pitch. The bar represents 10 μm.

tively on the structures, with 0 (S.D. 0) live and 0 (S.D. 0) dead cells on the surrounding silicon surfaces. In contrast, live *S. aureus* spread as single cells over the structures (6.25, S.D. 0.96) and surroundings (8.67, S.D. 3.51). Only one dead cell was found on the structured and none on the unstructured surfaces.

For a more comprehensive evaluation of the effect of various line array structures on the attachment of *E. coli* and *S. aureus* cells, fluorescence microscopy was employed after cell viability staining, with two sets of data images selected for further analysis (Fig. 5). The first set of data relates to fields where bacterial response to line distances of 600 nm, 800 nm, 1000 and 1200 nm with a constant line width of 400 nm were compared (Fig. 5A and B). The second set of data relates to fields where the line widths of 400 nm, 600 nm, 800 nm and 1000 nm was compared at constant line distance of 1200 nm (Fig. 5C and D). The line pitch at a constant line width of 400 nm had no significant effect on the adhesion of *E. coli* cells (Fig. 5A), which are relatively large (3 μm). There were five times less *E. coli* live cells than dead cells at all pitch distances. For *S. aureus* cells (Fig. 5B) the opposite was observed with a higher live cell attachment number and very few dead cells present. A slight increase of the number of live *S. aureus* cells could be observed with the increase of pitch.

The adhesion of live but not of dead *S. aureus* cells may be due to fact that only live *S. aureus* cells are capable of producing extra cellular substances which may facilitate adhesion, particularly for structures with wider groves (wider pitch) in which these cells may insert due to their relatively small size (500–600 nm). For line widths at constant pitch of 1200 nm no significant effect was seen with respect to the adhesion of live *E. coli* cells (Fig. 5C), whereas *S. aureus*, again with a higher live cell attachment number, showed a slight decrease of the number of cells with an increase of line width (Fig. 5D). *S. aureus* cells appear to preferentially adhere to the

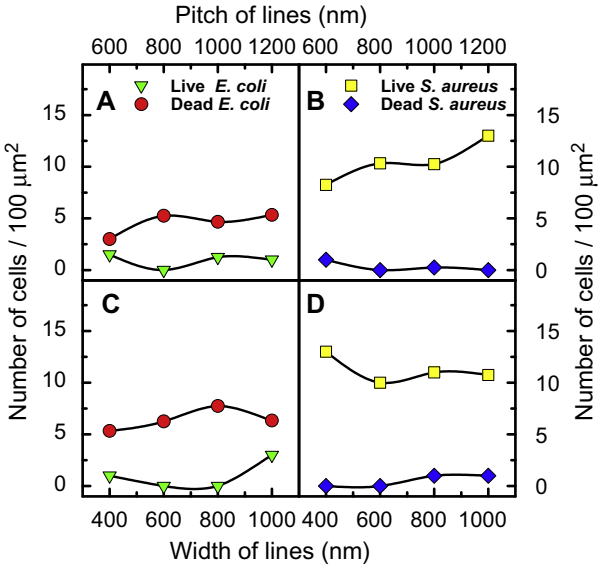

Fig. 5. Number of *E. coli* (A, C) or *S. aureus* (B, D) cells on 100 μm^2 of gold/silicon oxide nanostructured surfaces with either various line distances (pitch of 600 nm, 800 nm, 1000 nm and 1200 nm) at a constant line with of 400 nm (A, B) or with different line widths (400 nm, 600 nm, 800 nm and 1000 nm) at constant pitch of 1200 nm (C, D). The standard deviation of *E. coli* live and dead cells was <1.0 and <1.5, and that of *S. aureus* live and dead cells was <3.5 and <1.0, respectively.

wider grooves rather than to the gold protrusions [11], with the number of cells per 100 μm^2 substantially lower at suboptimal line widths. The preferential adhesion of *E. coli* on the nanostructures and their high mortality rate with such structured materials warrants further investigation.

4. Conclusion

The results show that cell viability on nanostructured surfaces was influenced by a combined effect of bacterial size, physiology and surface topography. A change of topography did not affect the adhesion of *E. coli* cells but for *S. aureus* cells changes in the dimensionality/width of the nanostructure caused an unusual preference for silicon groves over gold protrusions. The use of nanostructured arrays for the probing of bacteria-surface interactions, as exemplified in these investigations, may provide insights that will be useful for the manufacturing of 'designer' materials with pro- or anti-bacterial properties.

Acknowledgements

This project was supported by the Commonwealth of Australia under the International Science Linkages program and is related to the European-Australian integrated FP6 CHARPAN and FP7 BISNES project. The authors thank Gemma Rius Suñé, Xavier Borrise and Francesco Perez-Murano at the Centre Nacional de Microelectronica, CNM-IMB, CSIC, E-08193 Bellaterra, Spain for the provision of the nano-structured arrays.

References

[1] J. Li, L.A. Mclandsborough, Int. J. Food Microbiol. 53 (1999) 185–193.
[2] J.W. Costerton, P.S. Stewart, E.P. Greenberg, Science 284 (1999) 1318–1322.
[3] L. Hall-Stoodley, J.W. Costerton, P. Stoodley, Nat. Rev. Microbiol. 2 (2004) 95–108.
[4] A. Komaromy, R.I. Boysen, H. Zhang, I. McKinnon, F. Fulga, M.T.W. Hearn, D.V. Nicolau, Microelectron. Eng. 86 (2009) 1431–1434.
[5] S. Carnazza, C. Satriano, S. Guglielmino, G. Marletta, J. Colloid Interface Sci. 289 (2005) 386–393.
[6] E.P. Ivanova, Y.V. Alexeeva, D.K. Pham, J.P. Wright, Dan V. Nicolau, Int. Microbiol. 9 (2006) 37–46.
[7] E.P. Ivanova, D.V. Nicolau, N. Yumoto, T. Taguchi, K. Okamoto, Y. Tatsu, S. Yoshikawa, Mar. Biol. 130 (1998) 545–551.
[8] G. Colon, B.C. Ward, T.J. Webster, J. Biomed. Mater. Res. A 78A (3) (2006) 595–604.
[9] Baikun Li, Bruce E. Logan, Colloids Surf. B 36 (2004) 81–90.
[10] C. Satriano, G.M.L. Messina, S. Carnazza, S. Guglielmino, G. Marletta, Mater. Sci. Eng. A 26 (5–7) (2006) 942–946.
[11] S. Li, A.Z. Komaromy, D.V. Nicolau, R.I. Boysen, M.T.W. Hearn, Microelectron. Eng. 87 (2010) 715–718.